https://doi.org/10.5194/egusphere-2022-777
Preprint. Discussion started: 22 August 2022

Equilibrium climate sensitivity increases with aerosol concentration due to changes in rain efficiency

Guy Dagan[1*]

[1] Fredy and Nadine Herrmann Institute of Earth Sciences, Hebrew University, Jerusalem, Israel

*Corresponding author. Email: guy.dagan@mail.huji.ac.il

https://doi.org/10.5194/egusphere-2022-777
Preprint. Discussion started: 22 August 2022

Abstract

How Earth's climate reacts to anthropogenic forcing is one of the most burning questions faced by today's scientific community. A leading source of uncertainty in estimating this sensitivity is related to the response of clouds. Under the canonical climate-change perspective of forcings and feedbacks, the effect of anthropogenic aerosols on clouds is categorized under the forcing component, while the modifications of the radiative properties of clouds due to climate change are considered in the feedback component. Each of these components contributes the largest portion of uncertainty to its relevant category and is largely studied separately from the other. In this paper, using idealized cloud resolving, radiative-convective-equilibrium simulations, with a slab ocean model, we show that aerosol-cloud interactions could significantly affect cloud feedback. Specifically, we show that equilibrium climate sensitivity increases under high aerosol concentration due to an increase in the shortwave cloud feedback. The shortwave cloud feedback is enhanced under high aerosol conditions due to a stronger increase in the precipitation efficiency with warming, which can be explained by higher sensitivity of the droplet size and the cloud water content to the CO_2 concentration rise. These results indicate a strong connection between cloud feedback and aerosol-cloud interactions.

1. Introduction

Estimating Earth's equilibrium climate sensitivity (ECS), defined as the steady-state global mean temperature increase for a doubling of CO_2, is considered as a first-order, fundamental milestone on the way to understanding and predicting anthropogenic-driven climate change (Sherwood et al., 2020). Decades of research have tried to accurately quantify ECS, with only limited success. The most probable current ECS estimates are in the range of 2.3–4.5K (Sherwood et al., 2020). The largest source of uncertainty in estimating ECS is related to the response of clouds to the externally forced warming and the feedback of these changes on the climate system (Sherwood et al., 2020; Ceppi et al., 2017; Schneider et al., 2017). Clouds strongly modulate Earth's radiation budget by reflecting the incoming shortwave radiation from the sun and by absorbing and re-emitting the terrestrial longwave radiation (Loeb et al., 2018). Thus, changes in the cloud macro-physical properties (such as coverage and vertical extent) and micro-physical properties (such as liquid/ice partition or hydrometeors size) due to anthropogenic-driven climate change could significantly alter the climate system's response (Gettelman and Sherwood, 2016; Nuijens and Siebesma, 2019; Schneider et al., 2017).

An important factor in determining cloud feedback magnitude is the sensitivity of the Precipitation Efficiency (ϵ) (Lutsko et al., 2021; Li et al., 2022; Lutsko and Cronin, 2018). ϵ quantifies the fraction of condensed water in a cloud to reach the surface as precipitation. Using idealized cloud resolving simulations, it was shown that ϵ is expected to increase with temperature (Lutsko and Cronin, 2018). The increase in ϵ with warming was shown to be mostly driven by an increase in the efficiency with which cloud condensate is converted into precipitation, while changes in the evaporation of falling precipitation was shown to play a smaller role (Lutsko and Cronin, 2018).

An increase in ϵ with warming more efficiently depletes the water from the clouds, thus affecting the radiation budget. On the one hand, increase in ϵ with warming was suggested to reduce the anvil cloud coverage and hence increase the outgoing longwave radiation (Lindzen et al., 2001; Mauritsen and Stevens, 2015), thus producing negative feedback. On the other hand, however, it was recently shown that the longwave effect of an ϵ increase is over-compensated for by changes in the shortwave flux (Li et al., 2019), i.e., a large reduction in the cloud optical depth, driving a reduction in the shortwave cooling effect of clouds, dominates the response.

The efficiency with which cloud condensate is converted into precipitation is closely linked to the micro-physical properties of the clouds. The autoconversion of cloud droplets into rain becomes significant when liquid water amount and/or droplet radii reach a critical threshold (Freud and Rosenfeld, 2012). An important factor influencing the droplet radii (and also the liquid water amount, to some degree) is the amount of available cloud condensation nuclei (CCN). Generally, an increase in aerosol concentration drives an increase in CCN concentration, which results in more numerous and smaller droplets in the cloud (Twomey, 1974; Warner and Twomey, 1967). The smaller droplets require longer time (or equivalently larger vertical distance) in the clouds to grow by diffusion to the critical size enabling precipitation, thus delaying the initial warm rain formation (Rosenfeld, 2000; Dagan et al., 2015b). Therefore, aerosols could affect ϵ (Khain, 2009).

In addition to the effect on rain, aerosols could modify the radiative properties of clouds, by modifying the droplet concentration and size distribution (Twomey, 1974) and by affecting the clouds' macro-physical properties (Albrecht, 1989; Bellouin et al., 2019). These changes to the radiative properties of clouds result in radiative forcing that could affect the sea surface temperature [SST (Bellouin et al., 2019)]. Using cloud-resolving radiative-convective-equilibrium simulations with interactive SST, Khairoutdinov and Yang (2013) showed that the surface temperature decreases by 1.5K with each 10-fold increase in aerosol concentration, an effect quite comparable to a 2.1–2.3K SST warming obtained in a simulation with given (low) aerosol conditions but doubled CO_2 concentration.

It has been suggested that cloud feedback and aerosol forcing are not independent of each other (Mülmenstädt and Feingold, 2018; Igel and van den Heever, 2021). In addition, the strong links between ϵ and cloud feedback and between ϵ and aerosol concentration merit a dedicated study on the potential mutual CO_2 and aerosol effect on clouds and thus also on ECS, which is the aim of the current study.

2. Methods

Model description and experimental design

The model used herein is the System of Atmospheric Modeling [SAM - (Khairoutdinov and Randall, 2003)] version 6.11.7. Subgrid-scale fluxes are parameterized using Smagorinsky's eddy diffusivity model and gravity waves are damped at the top of the domain. The microphysics scheme used is Morrison et al. (2005) 2-moment bulk microphysics. The cloud droplet number concentration source assumes that the number of activated CCN depends on the super-saturation (S) according to a power-law: CDNC $= N_a S^k$, where N_a is the prescribed concentration of CCN active at 1 % supersaturation, and k is a constant (set in this study to 0.4 - a typical value for maritime conditions). Changes in N_a serve as a proxy for the change in aerosol concentration. Three levels of N_a are considered here, covering an extreme range of conditions – 20, 200 and 2000 cm^{-3}. While this wide range of conditions is unlikely to exist at any given geographical location, they are used here in order to cover the range of possible conditions at different locations and to maximize the effect for establishing better physical understanding. The activation of CCN at the cloud base is parameterized following Twomey (1959), using the vertical velocity and CCN spectrum parameters. The model computes cloud water and ice-crystal effective radius for the radiation; thus, the Twomey effect (Twomey,

https://doi.org/10.5194/egusphere-2022-777
Preprint. Discussion started: 22 August 2022

1977) of both liquid and ice is considered. Direct interactions between aerosols and radiation are not considered here.

The simulations are conducted in a radiative-convective-equilibrium (RCE) mode and generally follow the RCEMIP (RCE model inter-comparison project (Wing et al., 2018)) small-domain instructions (but with interactive SST and changes in the CO_2 and aerosol concentration). The simulations were performed on a square, doubly periodic domain. In this case, we want to avoid the effect of convective self-aggregation on ϵ; thus, the domain size is set to 96x96 km^2, which was shown to be small enough to prevent convective self-aggregation (Muller and Held, 2012; Lutsko and Cronin, 2018; Yanase et al., 2020). The horizontal grid spacing is set to 1km and 68 vertical levels are used, between 25m and 31km, with vertical grid spacing increasing from 50m near the surface to roughly 1km at the domain top. A time step of 10s is used, and radiative fluxes are calculated every 5 min using the CAM radiation scheme (Collins et al., 2006). The output resolution for all fields is 1h. The incoming solar radiation is fixed at 551.58 Wm^{-2} with a zenith angle of 42.05° (Wing et al., 2018), producing a net insolation close to the tropical-mean value. Convection is initialized with a small thermal noise added near the surface at the beginning of the simulation. The initial conditions for the simulations are as in Wing et al. (2018).

Greenhouse gases are varied for three different levels: pre-industrial level (280 PPM, 1xCO_2), 2 times pre-industrial level (2xCO_2) and 4 times pre-industrial level (4xCO_2). As in the case of the aerosol concentrations, the large range of CO_2 conditions covered here are used to examine the clouds' sensitivity to greenhouse gas concentrations under a wide range of conditions. Nine different simulations, with all possible combinations of N_a and CO_2 concentrations, were conducted.

In all simulations, the SST is interactive and predicted by a slab ocean model (SOM). The SOM's mixed layer depth is set to 5m, which represented a compromise between a relatively deep layer (≥10m), which reduces SST noise (Khairoutdinov and Yang, 2013), and a relatively shallow layer (≪1m), which requires a shorter computation time for equilibrium (Romps, 2020). As in Romps (2020), the SOM is cooled at a rate of 112 Wm^{-2} in order to ensure that the simulations with 1xCO_2 are kept at around the initial SST of 300K (Fig. 1). Each simulation was run for 1800 days, which is sufficient for reaching close to equilibrium (the surface energy imbalance is ≤0.1Wm^{-2} in all

https://doi.org/10.5194/egusphere-2022-777
Preprint. Discussion started: 22 August 2022

simulations during the last 150 days). The last 150 days of each run are used for statistical sampling (gray shading in Fig. 1).

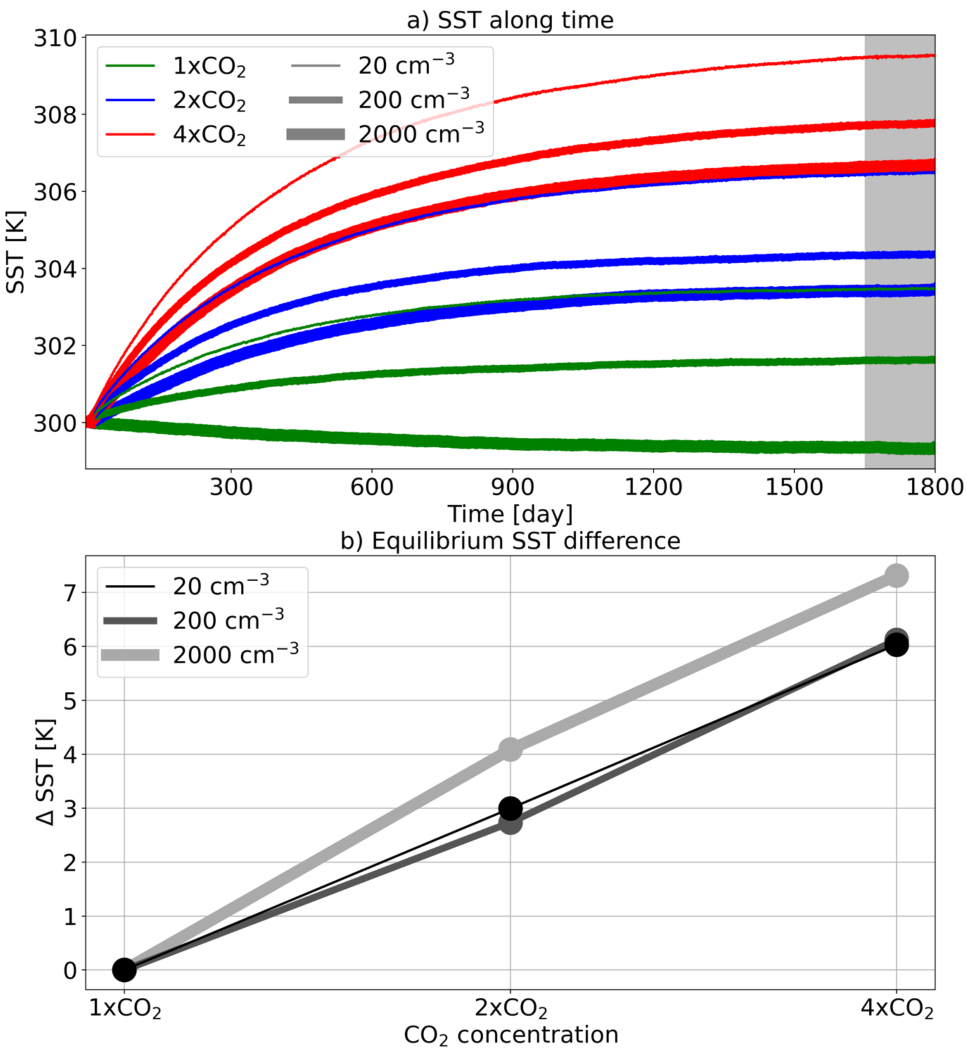

Figure 1. a) the sea surface temperature (SST) along time for the different simulations conducted under different aerosol and CO_2 concentrations. The gray shaded area is referred to as equilibrium conditions. b) Change in equilibrium SST due to a change in CO_2 concentration (compared to the $1xCO_2$ case of each aerosol concentration), for the different aerosol concentrations (the different curves).

https://doi.org/10.5194/egusphere-2022-777
Preprint. Discussion started: 22 August 2022

3. Results

Figure 1 presents the SST of the different simulations along time (panel a) and the change in the equilibrium SST with the CO_2 concentration for the different N_a cases (panel b). As expected, the equilibrium SST (gray shading in Fig. 1a) increases with the CO_2 concentration and decreases with N_a concentration. However, the rate of increase in equilibrium SST with CO_2 concentration increases under extremely high N_a concentrations (2000 cm^{-3}), compared with the low and medium N_a concentrations (20 and 200 cm^{-3}, respectively - Fig. 1b). Calculating the average ECS based on the three combinations available for each N_a condition [2xCO_2-1xCO_2, 4xCO_2-2xCO_2 and (4xCO_2-1xCO_2)/2], demonstrates that it increases with N_a from 3.0K at the lowest N_a to 3.7K at the highest N_a (i.e., a 23% increase – Table 1).

Table 1. Average equilibrium climate sensitivity (ECS), cloud-feedback parameter (λ_{cloud}), hydrological sensitivity (η), and change in precipitation efficiency ($\Delta\epsilon$) of the three combinations available for each N_a condition [2xCO_2-1xCO_2, 4xCO_2-2xCO_2 and 4xCO_2-1xCO_2]. For the calculation of the average ECS, the difference between 4xCO_2 and 1xCO_2 is divided by 2. The rest of the quantities are normalized by the SST change between the relevant simulations.

N_a [cm^{-3}]	ECS [K]	λ_{cloud} [W m^{-2} K^{-1}]	η [% K^{-1}]	$\Delta\epsilon$ [% K^{-1}]
20	3.0	-0.45	3.8	1.2
200	3.1	-0.38	4.3	1.3
2000	3.7	-0.08	4.6	2.7

Figure 2 presents the time and domain mean vertical profiles of temperature and water vapor mixing ratio (q_v) in the different simulations (panels a and b) and their difference from the simulation with the lowest N_a and CO_2 concentrations (panels c and d). It demonstrates, as expected, that the vertical profile of air temperature is set by the surface temperature (increases with CO_2 concentrations and decreases with N_a) with an amplification of the change at the upper troposphere, as the profiles follow the moist adiabatic lapse-rate. It also shows that q_c increases with the temperature, as expected (Held and Soden, 2006).

https://doi.org/10.5194/egusphere-2022-777
Preprint. Discussion started: 22 August 2022

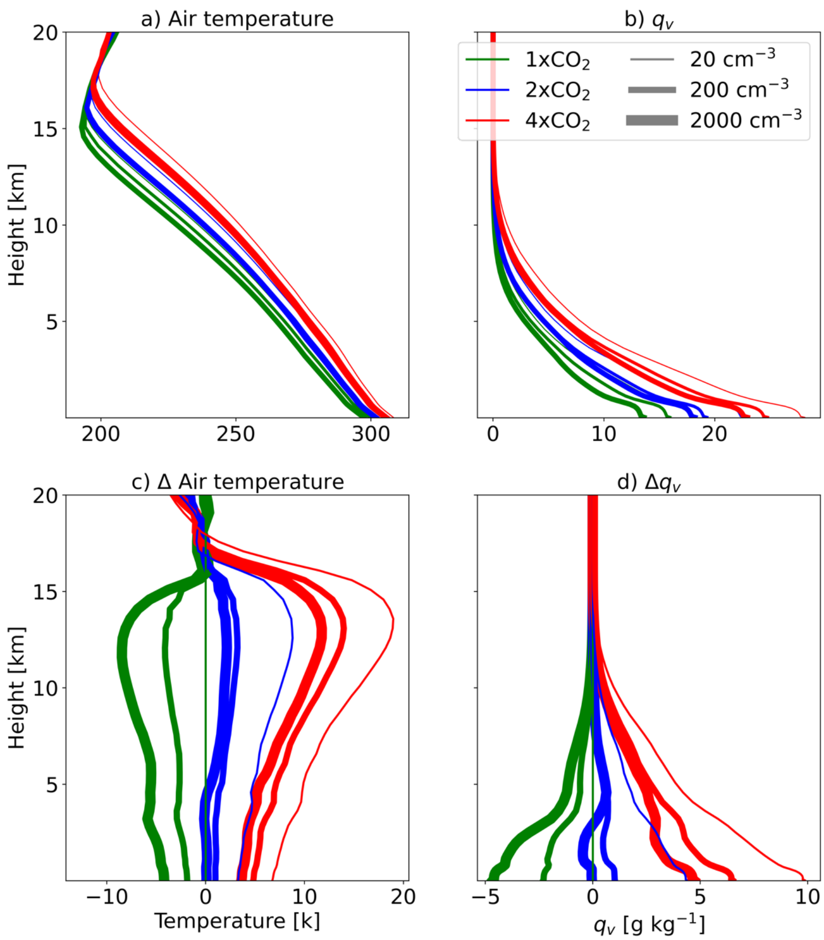

Figure 2. Time and domain mean vertical profiles of air temperature and water vapor mixing ratio (q_v) in the different simulations (a and b) and how they differ from the simulation with the lowest N_a and CO_2 concentrations (panels c and d).

In order to understand the increase in ECS with N_a, we next examine the top-of-atmosphere (TOA) energy budget. Figure 3 presents the change in the net shortwave and longwave TOA energy gain (R^{SW} and R^{LW}, respectively) with the CO_2 concentration for the different N_a conditions. In addition, Fig. 3 presents the change in the cloud radiative effect (CRE) with increasing the CO_2 concentration, where CRE is computed by subtracting the clear-sky from the all-sky TOA radiative fluxes ($R{-}R_{clear-sky}$), again for the shortwave and longwave separately (CRE^{SW} and CRE^{LW},

https://doi.org/10.5194/egusphere-2022-777
Preprint. Discussion started: 22 August 2022

respectively). Figure 3a and b demonstrates that under equilibrium conditions R^{SW} increases, while R^{LW} decreases with the CO_2 concentration. However, the rate of change in both R^{SW} and R^{LW} is much faster under the high N_a conditions than under the low and medium N_a conditions. The trend in $\mathrm{CRE}^{\mathrm{SW}}$ under the different N_a conditions (Fig. 3c) resembles the trend in R^{SW}, suggesting that the clouds' response dominates the changes in the TOA shortwave fluxes. $\mathrm{CRE}^{\mathrm{LW}}$, on the other hand, decreases at a similar rate with CO_2 concentration for the different N_a conditions (Fig. 3d). Thus, the different decrease rates in R^{LW} with CO_2 concentration for the different N_a conditions (Fig. 3b) must be driven by clear-sky changes (specifically, the plank and the lapse-rate feedbacks – see Fig. 2 above).

In Table 1 above, we estimate the average cloud radiative feedback (λ_{cloud}) as the change in CRE with increasing surface temperature, i.e., $\lambda_{\mathrm{cloud}} = d\mathrm{CRE}/dT$, for the different N_a conditions. The table shows that λ_{cloud} becomes less negative with the increase in N_a, leading to higher climate sensitivity. The differences in the values of λ_{cloud} between the different N_a conditions is mostly derived from the shortwave part of the spectrum (Fig. 3).

https://doi.org/10.5194/egusphere-2022-777
Preprint. Discussion started: 22 August 2022

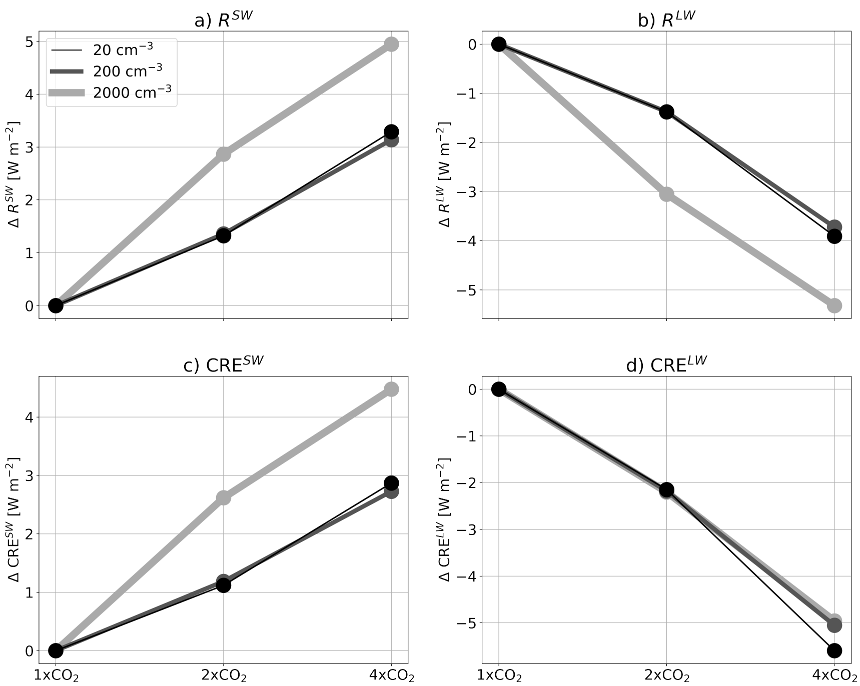

Figure 3. The change in the net top-of-atmosphere energy gain (*R*) in the shortwave (a) and in the longwave (b), and the change in the cloud radiative effect (CRE) in the shortwave (c) and in the longwave (d), due to a change in the CO_2 concentration (compared to the 1xCO_2 case of each aerosol concentration), for the different aerosol concentrations (the different curves).

Thus far, we have seen that the ECS increases with N_a (Fig. 1 and Table 1) and that this increase can be explained by changes in λ_{cloud} (Table 1) and specifically in CRE^{SW} (Fig. 3). To understand the changes in the cloud properties driving the changes in λ_{cloud}, and hence also in ECS, under the different N_a conditions, in Fig. 4 we present the change in cloud liquid water path (CWP), ice water path (IWP), rain water path (RWP) and cloud fraction (CF) with increasing CO_2 concentrations for the different N_a conditions. The figure shows that the CWP decreases with the CO_2 concentrations at a much faster rate (about 3 times faster) under the highest N_a conditions compared to the low and medium N_a conditions (Fig. 4a). The changes in the IWP, on the other hand, are about an order of magnitude smaller than the changes in CWP and are not consistent in sign for the different N_a conditions (Fig. 4b). The RWP increases with the CO_2 concentrations at a slightly faster rate (about 20% faster) under the highest N_a conditions compared to the

https://doi.org/10.5194/egusphere-2022-777
Preprint. Discussion started: 22 August 2022

low and medium N_a conditions (however the response is non-monotonic with N_a - Fig. 4c). The CF decreases with the CO_2 concentrations, at a similar rate for the different N_a conditions (about 1.5% decrease in CF for each doubling of the CO_2 concentrations - Fig. 4d).

The faster decrease in CWP with CO_2 concentrations under high N_a conditions drives the faster increase in CRE^{SW} as the clouds become less opaque in the shortwave. We note that the difference in CRE^{SW} trend under different N_a conditions could not be explained by the minor differences in the CF trends. In addition, the small differences in the IWP between the different N_a conditions are consistent with the small differences in the CRE^{LW} seen above. The general increase in RWP with CO_2 concentrations is consistent with an increase in rain efficiency with warming (Lutsko and Cronin, 2018), as elaborated below.

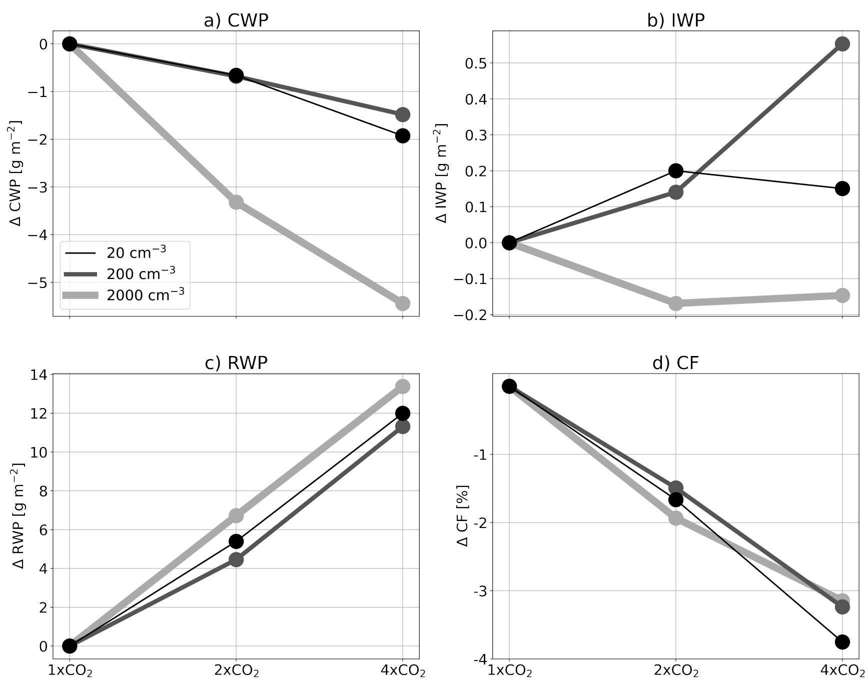

Figure 4. The change in: a) cloud liquid water path (CWP), b) ice water path (IWP, c) rain water path (RWP), and d) cloud fraction (CF) due to a change in the CO_2 concentration (compared to the $1xCO_2$ case of each aerosol concentration), for the different aerosol concentrations (the different curves).

https://doi.org/10.5194/egusphere-2022-777
Preprint. Discussion started: 22 August 2022

Figure 4 suggests that the largest difference in the cloud response to CO_2 under different N_a conditions is due to changes in CWP. The higher sensitivity of CWP to CO_2 concentration under higher N_a conditions can explain the higher λ_{cloud} and thus also the larger ECS. Hence, the question arises: What causes the faster reduction in CWP with CO_2 concentration under high N_a conditions? A major sink for CWP is via precipitation. Hence, in Fig. 5 we present the change in the mean surface precipitation rate, the hydrological sensitivity (η - the rate of change in the surface precipitation per 1K increase in surface temperature) and the precipitation efficiency (ϵ- calculated following Li et al. (2022) as the ratio of surface precipitation-to-condensed water path, i.e., CWP+IWP+RWP). As expected, the surface precipitation increases with CO_2 (i.e., η is positive) and so does ϵ (Lutsko and Cronin, 2018). This is true for all N_a conditions. However, the rates of increase in surface precipitation and ϵ with CO_2 concentration are higher under the highest N_a conditions (see also Table 1). We note that the larger rate of increase in surface precipitation under the highest N_a conditions is not solely due to the higher surface temperature increase, as η also increases with N_a.

The much larger (more than double- Table 1) rate of increase in ϵ with the CO_2 concentration under the highest N_a conditions depletes the cloud water more efficiently from the atmosphere, leading to a faster reduction in CWP with CO_2 concentration (Fig. 4), which in turn leads to higher λ_{cloud} and ECS. The faster increase in RWP with CO_2 concentration under the highest N_a conditions presented in Fig. 4c is consistent with this explanation.

https://doi.org/10.5194/egusphere-2022-777
Preprint. Discussion started: 22 August 2022

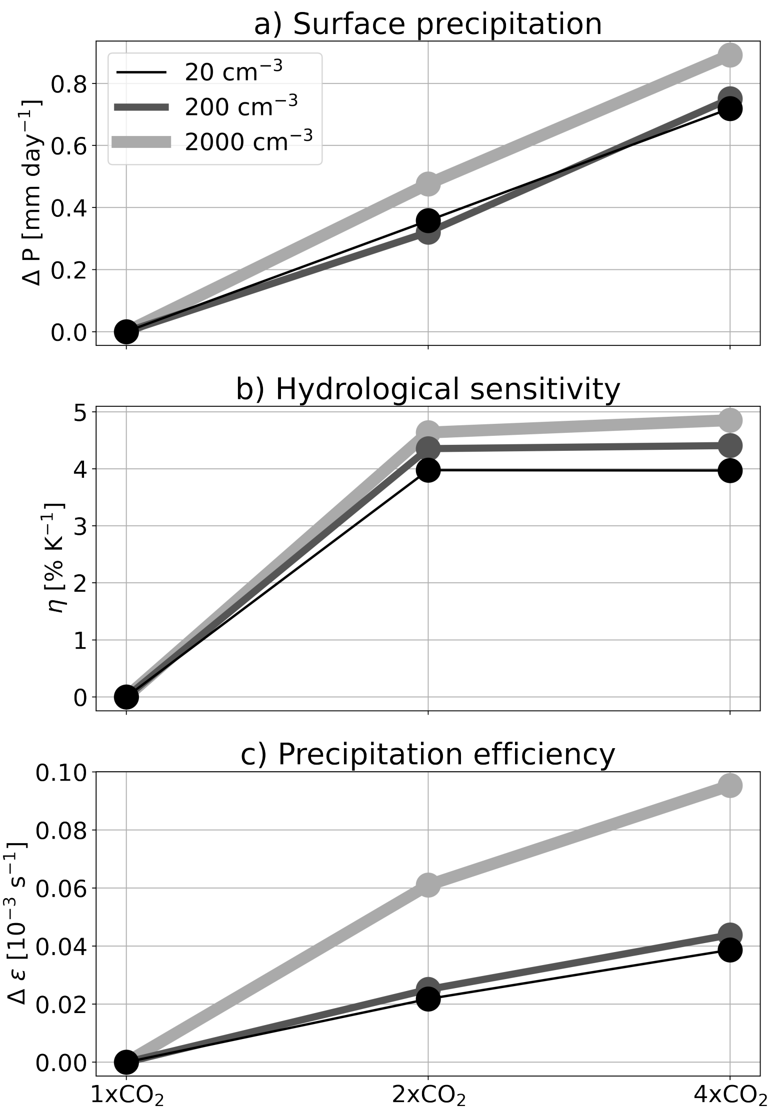

Figure 5. The change in: a) surface precipitation, b) hydrological sensitivity (η), and c) precipitation efficiency (ϵ) due to a change in the CO_2 concentration (compared to the 1xCO_2 case of each aerosol concentration), for the different aerosol concentrations (the different curves).

The last open question is why ϵ increases faster with CO_2 concentration under the highest N_a conditions. The increase in ϵ with warming was shown to be mostly driven by an increase in the efficiency with which cloud condensate is converted into

https://doi.org/10.5194/egusphere-2022-777
Preprint. Discussion started: 22 August 2022

precipitation (Lutsko and Cronin, 2018). As was mentioned in the introduction, the conversion of cloud condensate into precipitation (or autoconversion of cloud droplets) becomes significant only when liquid water amount and/or droplet radii reach a critical threshold (Freud and Rosenfeld, 2012). To understand the faster ϵ increases with CO_2 concentration under the highest N_a conditions, we present the histograms over the domain and time (during the last 150 days of the simulations based on 3D output in 1-hour resolution) of liquid cloud droplets mixing ratio (q_c – Fig. 6) and mean cloud droplet radii ($\overline{r_c}$ – Fig. 7) around the height of the maximum in cloud droplet effective radii (1950m) and its mean sensitivity to doubling of CO_2 concentration for each N_a condition.

Figure 6 demonstrates that the cut-off of the q_c distribution (the mixing ratio for which the probability density function starts to decrease sharply) increases with the CO_2 concentration and decreases with the aerosol concentration. However, the sensitivity of the relatively large q_c with CO_2 concentration is significantly larger under high aerosol concentrations compared to the lower aerosol concentrations (Fig. 6b). The larger relative increase in high q_c promotes the autoconversion process and hence enhances ϵ, more under high aerosol concentrations than under low aerosol concentrations.

Figure 7 demonstrates, in line with expectations, that N_a has a strong effect on $\overline{r_c}$. In addition, it shows that under all N_a conditions, $\overline{r_c}$ increases with the CO_2 concentration. This could be explained by the increase in the availability of water vapor (Fig. 2), which, for a given N_a conditions, enable larger diffusional growth of the droplets. Here again, the highest N_a conditions demonstrate the largest sensitivity of $\overline{r_c}$ to CO_2 concentration, especially at the right-hand side of the distribution (Fig. 7b). This could be explained by the fact that under these high N_a conditions, the cloud droplet growth is primarily limited by the availability of water vapor, as large number of droplets compete for the available water vapor (Koren et al., 2014; Dagan et al., 2015a; Reutter et al., 2009). Similarly to the q_c case, the larger relative increase in the relatively large droplets promotes the autoconversion process and hence enhances ϵ, more under high aerosol concentrations than under lower aerosol concentrations.

https://doi.org/10.5194/egusphere-2022-777
Preprint. Discussion started: 22 August 2022

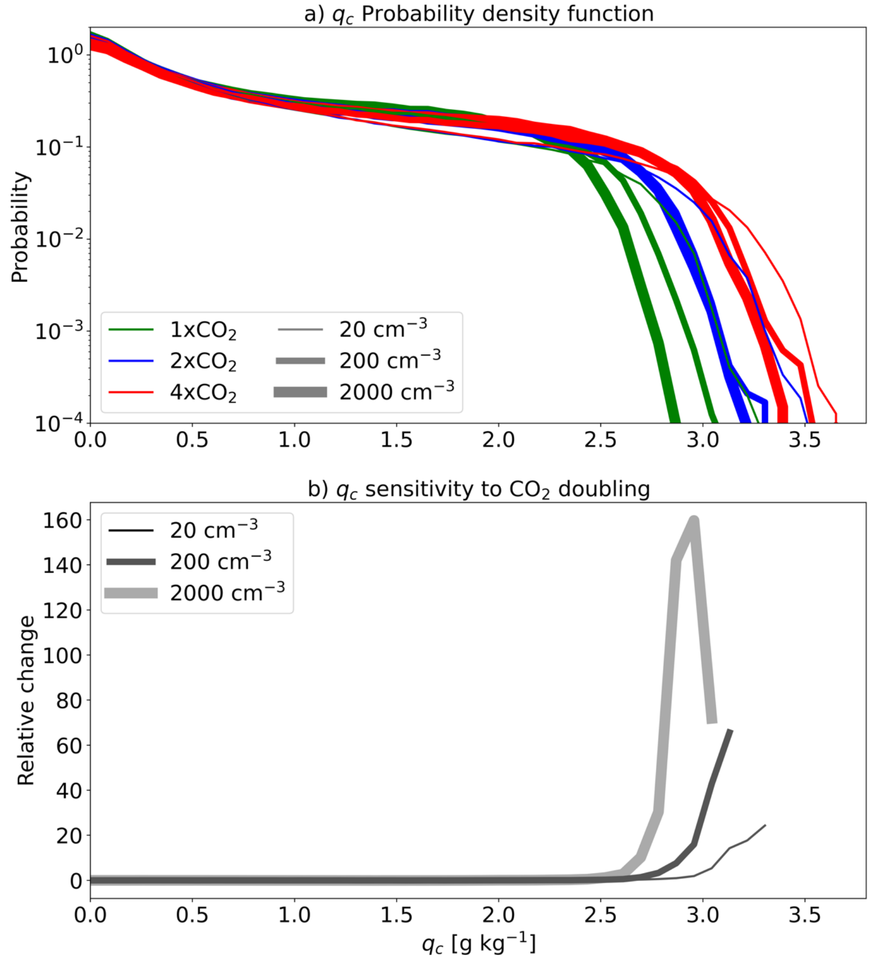

Figure 6. Probability density functions (PDF) of the cloud droplet mixing ratio (q_c) for the different simulations (a), and the mean sensitivity of the q_c PDF to a doubling of the CO_2 concentration based on the three combinations available for each N_a condition [2xCO_2-1xCO_2, 4xCO_2-2xCO_2 and (4xCO_2-1xCO_2)/2] (b), calculated for the heights around which the cloud droplet effective radii reach a maximum (1950m) and using 3-D files output every hour of the last 150 days of the simulations. Note the logarithmic scales for the y-axes of a.

https://doi.org/10.5194/egusphere-2022-777
Preprint. Discussion started: 22 August 2022

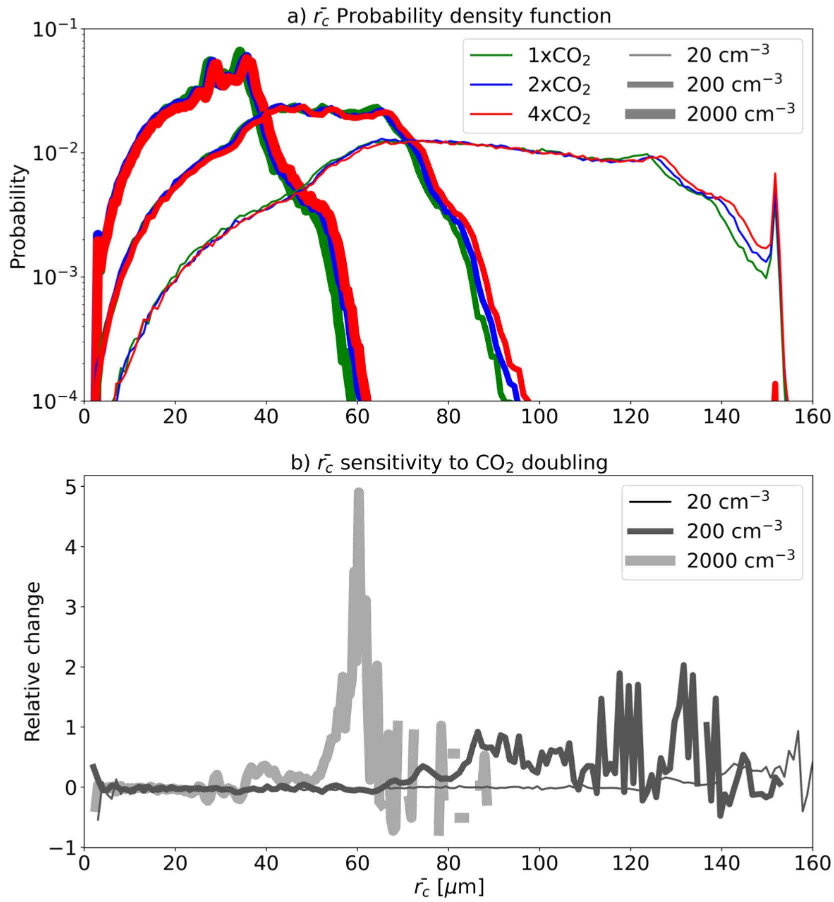

Figure 7. Probability density functions (PDF) of cloud droplet mean radii ($\overline{r_c}$) for the different simulations (a), and the mean sensitivity of the $\overline{r_c}$ PDF to a doubling of the CO_2 concentration based on the three combinations available for each N_a condition [2xCO_2-1xCO_2, 4xCO_2-2xCO_2 and (4xCO_2-1xCO_2)/2] (b), calculated for the heights around which the cloud droplet effective radii reach a maximum (1950m) and using 3-D files output every hour of the last 150 days of the simulations. Note the logarithmic scales for the y-axes of a.

4. Summary and conclusions

The role of clouds in a climate-change is manifested by two pathways: (1) effects of anthropogenic aerosol on clouds, and (2) feedback that clouds exert on the changing climate. These two pathways are usually studied separately, and even by different

https://doi.org/10.5194/egusphere-2022-777
Preprint. Discussion started: 22 August 2022

scientific communities. In this paper, we demonstrate that the two pathways are closely linked to each other and should be examined concurrently.

Using long, idealized RCE simulations over a small domain with a slab ocean model, we demonstrate that the ECS, i.e., the increase in surface temperature under equilibrium conditions due to doubling of the CO_2 concentration, increases with the aerosol concentration. The ECS increase is explained by a faster increase in precipitation efficiency with warming under high aerosol concentrations, which more efficiently depletes the water from the cloud and thus is manifested as an increase in the cloud feedback parameter. The precipitation efficiency increases faster under high aerosol concentration due to a higher sensitivity of the relatively high liquid water mixing ratios and the relatively large mean droplet sizes to a CO_2 concentration increase.

The results presented here are based on idealized simulations over a small domain. Under more realistic conditions, other processes, not included here, that could affect the precipitation efficiency and hence the general trend will be introduced. In particular, convective self-aggregation could be of interest as, while it is inhibited in the small domain used here, it was shown to affect precipitation efficiency (Lutsko et al., 2021) and to be affected by aerosols (Nishant et al., 2019). Other processes that should be accounted for in future research include the presence of large-scale circulation and direct aerosol radiative effects (Dagan et al., 2019; Dingley et al., 2021).

The results presented here suggest a strong connection between cloud feedback and aerosol-cloud interactions. The regulation of aerosol emissions is known to be more effective than the effort to reduce greenhouse gas emissions. This, together with the short lifetime of aerosols in the atmosphere, has resulted in a reduction in the value of the global mean aerosol effective radiative forcing in recent years (Quaas et al., 2022). If the conclusions of this paper hold under higher levels of complexity (e.g., large-scale circulation, convective self-aggregation, etc.) this might mean that the reduction in global aerosol emissions could lead to a reduction in ECS, which could compensate, at least partially, for the reduction in the negative forcing induced by aerosols (Quaas et al., 2022; Bellouin et al., 2019), thus providing yet additional motivation for reducing aerosol emissions globally.

Code availability

SAM is publicly available at: http://rossby.msrc.sunysb.edu/~marat/SAM.html

https://doi.org/10.5194/egusphere-2022-777
Preprint. Discussion started: 22 August 2022

Data availability

The data presented in this study will become publicly available via zenodo prior to publication.

Author contributions

GD carried out the simulations and analyses presented and prepared the article.

Competing interests

The authors declare that they have no conflict of interest.

Financial support

This research was supported by the Israeli Science Foundation Grant (1419/21).

5. References

Albrecht, B. A.: Aerosols, cloud microphysics, and fractional cloudiness, Science (New York, NY), 245, 1227, 1989.

Bellouin, N., Quaas, J., Gryspeerdt, E., Kinne, S., Stier, P., Watson-Parris, D., Boucher, O., Carslaw, K., Christensen, M., and Daniau, A.-L.: Bounding aerosol radiative forcing of climate change, Reviews of Geophysics, 2019.

Ceppi, P., Brient, F., Zelinka, M. D., and Hartmann, D. L.: Cloud feedback mechanisms and their representation in global climate models, WIREs Climate Change, 2017.

Collins, W. D., Rasch, P. J., Boville, B. A., Hack, J. J., McCaa, J. R., Williamson, D. L., Briegleb, B. P., Bitz, C. M., Lin, S.-J., and Zhang, M.: The formulation and atmospheric simulation of the Community Atmosphere Model version 3 (CAM3), Journal of Climate, 19, 2144-2161, 2006.

Dagan, G., Koren, I., and Altaratz, O.: Competition between core and periphery-based processes in warm convective clouds–from invigoration to suppression, Atmospheric Chemistry and Physics, 15, 2749-2760, 2015a.

Dagan, G., Koren, I., and Altaratz, O.: Aerosol effects on the timing of warm rain processes, Geophysical Research Letters, 42, 4590-4598, 10.1002/2015GL063839, 2015b.

Dagan, G., Stier, P., and Watson-Parris, D.: Contrasting response of precipitation to aerosol perturbation in the tropics and extra-tropics explained by energy budget considerations, Geophysical Research Letters, 2019.

Dingley, B., Dagan, G., and Stier, P.: Forcing convection to aggregate using diabatic heating perturbations, Journal of Advances in Modeling Earth Systems, 13, e2021MS002579, 2021.

Freud, E., and Rosenfeld, D.: Linear relation between convective cloud drop number concentration and depth for rain initiation, Journal of Geophysical Research: Atmospheres (1984–2012), 117, 2012.

Gettelman, A., and Sherwood, S.: Processes Responsible for Cloud Feedback, Current Climate Change Reports, 2, 179-189, 2016.

https://doi.org/10.5194/egusphere-2022-777
Preprint. Discussion started: 22 August 2022

Held, I. M., and Soden, B. J.: Robust responses of the hydrological cycle to global warming, Journal of Climate, 19, 5686-5699, 2006.

Igel, A. L., and van den Heever, S. C.: Invigoration or Enervation of Convective Clouds by Aerosols?, Geophysical Research Letters, 48, e2021GL093804, 2021.

Khain, A. P.: Notes on state-of-the-art investigations of aerosol effects on precipitation: a critical review, Environmental Research Letters, 4, 015004 (015020 pp.)-015004 (015020 pp.), 10.1088/1748-9326/4/1/015004, 2009.

Khairoutdinov, M., and Yang, C.-E.: Cloud-resolving modelling of aerosol indirect effects in idealised radiative-convective equilibrium with interactive and fixed sea surface temperature, Atmospheric Chemistry and Physics, 13, 4133-4144, 2013.

Khairoutdinov, M. F., and Randall, D. A.: Cloud resolving modeling of the ARM summer 1997 IOP: Model formulation, results, uncertainties, and sensitivities, Journal of the Atmospheric Sciences, 60, 2003.

Koren, I., Dagan, G., and Altaratz, O.: From aerosol-limited to invigoration of warm convective clouds, science, 344, 1143-1146, 2014.

Li, R., Storelvmo, T., Fedorov, A. V., and Choi, Y.-S.: A positive IRIS feedback: Insights from climate simulations with temperature-sensitive cloud–rain conversion, Journal of climate, 32, 5305-5324, 2019.

Li, R. L., Studholme, J. H., Fedorov, A. V., and Storelvmo, T.: Precipitation efficiency constraint on climate change, Nature Climate Change, 12, 642-648, 2022.

Lindzen, R. S., Chou, M.-D., and Hou, A. Y.: Does the earth have an adaptive infrared iris?, Bulletin of the American Meteorological Society, 82, 417-432, 2001.

Loeb, N. G., Doelling, D. R., Wang, H., Su, W., Nguyen, C., Corbett, J. G., Liang, L., Mitrescu, C., Rose, F. G., and Kato, S.: Clouds and the earth's radiant energy system (CERES) energy balanced and filled (EBAF) top-of-atmosphere (TOA) edition-4.0 data product, Journal of Climate, 31, 895-918, 2018.

Lutsko, N., Sherwood, S. C., and Zhao, M.: Precipitation Efficiency and Climate Sensitivity (Invited Chapter for the AGU Geophysical Monograph Series" Clouds and Climate"), 2021.

Lutsko, N. J., and Cronin, T. W.: Increase in precipitation efficiency with surface warming in radiative-convective equilibrium, Journal of Advances in Modeling Earth Systems, 10, 2992-3010, 2018.

Mauritsen, T., and Stevens, B.: Missing iris effect as a possible cause of muted hydrological change and high climate sensitivity in models, Nature Geoscience, 8, 346, 2015.

Morrison, H., Curry, J., and Khvorostyanov, V.: A new double-moment microphysics parameterization for application in cloud and climate models. Part I: Description, Journal of the atmospheric sciences, 62, 1665-1677, 2005.

Muller, C. J., and Held, I. M.: Detailed investigation of the self-aggregation of convection in cloud-resolving simulations, Journal of the Atmospheric Sciences, 69, 2551-2565, 2012.

Mülmenstädt, J., and Feingold, G.: The Radiative Forcing of Aerosol–Cloud Interactions in Liquid Clouds: Wrestling and Embracing Uncertainty, Current Climate Change Reports, 4, 23-40, 2018.

Nishant, N., Sherwood, S. C., and Geoffroy, O.: Aerosol-induced modification of organised convection and top-of-atmosphere radiation, npj Climate and Atmospheric Science, 2, 1-10, 2019.

Nuijens, L., and Siebesma, A. P.: Boundary Layer Clouds and Convection over Subtropical Oceans in our Current and in a Warmer Climate, Current Climate Change Reports, 1-15, 2019.

https://doi.org/10.5194/egusphere-2022-777
Preprint. Discussion started: 22 August 2022

Quaas, J., Jia, H., Smith, C., Albright, A. L., Aas, W., Bellouin, N., Boucher, O., Doutriaux-Boucher, M., Forster, P. M., and Grosvenor, D.: Robust evidence for reversal in the aerosol effective climate forcing trend, Atmospheric Chemistry and Physics Discussions, 1-25, 2022.

Reutter, P., Su, H., Trentmann, J., Simmel, M., Rose, D., Gunthe, S., Wernli, H., Andreae, M., and Pöschl, U.: Aerosol-and updraft-limited regimes of cloud droplet formation: influence of particle number, size and hygroscopicity on the activation of cloud condensation nuclei (CCN), Atmospheric Chemistry and Physics, 9, 7067-7080, 2009.

Romps, D. M.: Climate sensitivity and the direct effect of carbon dioxide in a limited-area cloud-resolving model, Journal of Climate, 33, 3413-3429, 2020.

Rosenfeld, D.: Suppression of rain and snow by urban and industrial air pollution, Science, 287, 1793-1796, 10.1126/science.287.5459.1793, 2000.

Schneider, T., Teixeira, J., Bretherton, C. S., Brient, F., Pressel, K. G., Schär, C., and Siebesma, A. P.: Climate goals and computing the future of clouds, Nature Climate Change, 7, 3-5, 2017.

Sherwood, S., Webb, M. J., Annan, J. D., Armour, K., Forster, P. M., Hargreaves, J. C., Hegerl, G., Klein, S. A., Marvel, K. D., and Rohling, E. J.: An assessment of Earth's climate sensitivity using multiple lines of evidence, Reviews of Geophysics, 58, e2019RG000678, 2020.

Twomey, S.: The nuclei of natural cloud formation part II: The supersaturation in natural clouds and the variation of cloud droplet concentration, Geofisica pura e applicata, 43, 243-249, 1959.

Twomey, S.: Pollution and the planetary albedo, Atmospheric Environment (1967), 8, 1251-1256, 1974.

Twomey, S.: The influence of pollution on the shortwave albedo of clouds, Journal of the atmospheric sciences, 34, 1149-1152, 1977.

Warner, J., and Twomey, S.: The production of cloud nuclei by cane fires and the effect on cloud droplet concentration, Journal of the atmospheric Sciences, 24, 704-706, 1967.

Wing, A. A., Reed, K. A., Satoh, M., Stevens, B., Bony, S., and Ohno, T.: Radiative-convective equilibrium model intercomparison project, Geoscientific Model Development, 793-813, 2018.

Yanase, T., Nishizawa, S., Miura, H., Takemi, T., and Tomita, H.: New critical length for the onset of self-aggregation of moist convection, Geophysical Research Letters, 47, e2020GL088763, 2020.